Fluorescent probes for selective protein labeling in lysosomes: a case of α-galactosidase A

Cornelius Bohl,* Adam Pomorski,† Susanne Seemann,* Anne-Marie Knospe,* Chaonan Zheng,* Artur Krężel,† Arndt Rolfs,* and Jan Lukas*,[1]

*Albrecht-Kossel-Institute for Neuroregeneration, Rostock University Medical Center, Rostock, Mecklenburg-Vorpommern, Germany; and †Department of Chemical Biology, Faculty of Biotechnology, University of Wroclaw, Wrocław, Poland

ABSTRACT: Fluorescence-based live-cell imaging (LCI) of lysosomal glycosidases is often hampered by unfavorable pH and redox conditions that reduce fluorescence output. Moreover, most lysosomal glycosidases are low-mass soluble proteins that do not allow for bulky fluorescent protein fusions. We selected α-galactosidase A (GALA) as a model lysosomal glycosidase involved in Anderson-Fabry disease (AFD) for the current LCI approach. Examination of the subcellular localization of AFD-causing mutants can reveal the mechanism underlying cellular trafficking deficits. To minimize genetic GALA modification, we employed a biarsenical labeling protocol with tetracysteine (TC-tag) detection. We tested the efficiency of halogen substituted biarsenical probes to interact with C-terminally TC-tagged GALA peptide at pH 4.5 *in vitro* and identified F2FlAsH-EDT$_2$ as a superior detection reagent for GALA. This probe provides improved signal/noise ratio in labeled COS-7 cells transiently expressing TC-tagged GALA. The investigated fluorescence-based LCI technology of TC-tagged lysosomal protein using an improved biarsenical probe can be used to identify novel compounds that promote proper trafficking of mutant GALA to lysosomal compartments and rescue the mutant phenotype.—Bohl, C., Pomorski, A., Seemann, S., Knospe, A.-M., Zheng, C., Krężel, A., Rolfs, A., Lukas, J. Fluorescent probes for selective protein labeling in lysosomes: a case of α-galactosidase A. FASEB J. 31, 000–000 (2017). www.fasebj.org

KEY WORDS: Anderson-Fabry disease · protein trafficking · live-cell imaging · biarsenical probes · tetracysteine tag

Live-cell imaging (LCI) is the method of choice for exploring dynamic cellular activities. For example, LCI has been applied to investigate biologic processes like cell migration (1, 2), morphologic changes of cells (3, 4), and even very fast and complex processes like membrane trafficking, vesicle formation, and signal transduction (5, 6) in numerous cellular contexts. A resolution of as little as 20 nm can be achieved with super-resolution techniques, such as standard emission depletion, stochastic optical reconstruction, and photoactivated localization (7). To determine transport and location of proteins in the cellular context, fluorescent protein (FP) fusions are widely used in LCI. Advantages of this technique include facile genetically engineered ectopic expression and specific stoichiometric labeling of tagged proteins. In addition to a broad fluorescence spectrum ranging from ultraviolet to deep red, some of the FPs have the ability to change spectrum upon irradiation (photoactivatable and switchable FPs). The availability of coral-derived FPs with relatively low pK_a also enables use in acidic cell compartments such as the lysosome (8). However, there are some major disadvantages. FP-fusion proteins may be altered in expression, folding, and subcellular localization (9, 10) and function (11, 12), warranting investigation of more suitable LCI methods for the examination of misfolded proteins and endoplasmic reticulum (ER)–associated degradation (ERAD) related to disease. The use of synthetic fluorophores was recently proposed, and optimization of low-molecular-weight tags, brighter fluorophores, and increased photostability offered a superior imaging system compared to FPs in super-resolution LCI (13).

ABBREVIATIONS: BA, barrier filter; DM, dichroic mirror; Dox, doxycycline; EDT, 1,2-ethanedithiol; Endo H, endoglycosidase H; ERAD, endoplasmic reticulum–associated degradation; EX, excitation filter; FlAsH, fluorescein arsenical helix/hairpin binder; FP, fluorescent protein; GALA, α-galactosidase A; GALA-TC, α-galactosidase A with tetracysteine tag; LAMP2, lysosome-associated membrane protein 2; LCI, live-cell imaging; PC, pharmacological chaperone; RFP, red fluorescent protein; ROI, region of interest; TBP, tributylphosphine; TCEP, *tris*(2-carboxyethyl)phosphine; TFA, trifluoroacetic acid

[1] Correspondence: Albrecht-Kossel-Institute for Neuroregeneration, Rostock University Medical Center, Gehlsheimer Straße 20, Rostock, Mecklenburg-Vorpommern 18147, Germany. E-mail: jan.lukas@med.uni-rostock.de

doi: 10.1096/fj.201700058RRRR
This article includes supplemental data. Please visit *http://www.fasebj.org* to obtain this information.

In this study, we used lysosomal α-galactosidase A [GALA, Online Mendelian Inheritance in Man (OMIM) *300644, EC 3.2.1.22], a representative lysosomal glycosidase involved in human disease (OMIM 301500) to establish an LCI protocol that monitors proteins located within the lysosomal lumen. The oxidative redox potential and acidic conditions complicate LCI of proteins located to this compartment. GALA was genetically fused to a tetracysteine (TC) tag (14), to allow for specific labeling using membrane-permeable biarsenical ligands that become highly fluorescent upon binding (Supplemental Fig. 1*A*). This technique has been used in multiple studies to track different proteins in living cells (15). However, there is no study reporting a successful implementation of this technique for visualizing intralysosomal proteins. Recently, the biarsenical fluorescein arsenical helix-to-hairpin binder-1,2-ethanedithiol (FlAsH-EDT_2) and 7 analogs have been described as differing in their physicochemical properties, revealing, for example, improved properties of the halogen-substituted probes, considering the pH-dependent fluorescence (16).

GALA is encoded by the X-chromosomal *GLA* gene (Xq22.1) and mutations within the gene lead to Anderson-Fabry disease (AFD), a hereditary metabolic disorder of glycosphingolipid storage. The enzyme catalyzes the removal of terminal α-galactose moieties from macromolecules such as glycopeptides and glycolipids (17). GALA is synthesized and folded inside the ER, glycosylated, transported to the Golgi apparatus, and finally processed to the endosomal/lysosomal system. Several hundred mutations have been described so far. A large number of mutant variants cause folding and stability defects, which in turn lead to premature proteasomal degradation of the corresponding enzyme (18–21). Although the failure to traffic along the endocytic route to the lysosome is an important indicator for the molecular damage of mutant GALA, the specific mechanism of the transport and degradation kinetics are not entirely known. We selected GALA as a paradigmatic medium-sized soluble lysosomal protein for a proof-of-concept study of organelle trafficking using TC-tag based fluorophore labeling. To this end, we performed an initial screening of biarsenical probes with a peptide consisting of C-terminal GALA with an optimized TC-tag (22) ($GALA^{412–429}$TC) for *in vitro* labeling. Subsequently, C-terminal TC-tagged GALA (GALA-TC) was generated and expressed and visualized in COS-7 cells. We compared the fluorescence level of complexes with $GALA^{412–429}$TC for conventional FlAsH to 4 recently characterized biarsenical probes with lower pK_a of the 3′-hydroxyl group (Supplemental Fig. 1*B*) to demonstrate that biarsenical probes are capable of labeling tagged proteins in acidic compartment. The optimized biarsenical compounds showed improved binding characteristics *in vitro* and are excellent for visualizing lysosomal GALA *in situ*. LCI can be used to investigate the cellular fate of novel gene mutations in diseases such as AFD and to elucidate cellular degradation and trafficking defects of proteins involved in lysosomal storage diseases.

MATERIALS AND METHODS

Materials

All DNA oligos were ordered form MWG Eurofins (Martinsried, Germany). All chemicals used in this study were obtained from Millipore-Sigma (Crailsheim, Germany), IRIS Biotech (Marktredwitz, Germany), or Avantor Performance Materials (Gliwice, Poland) unless indicated otherwise. Tenta Gel resin was from Rapp Polymere (Tübingen, Germany).

Synthesis of the GALA model peptide

Tetracysteine peptide NH_2-TVLLQLENTMQMSLKDLL*FLNC-CPGCCMEP*-amide ($GALA^{412–429}$TC) constituting the C-terminal part of human GALA with optimized TC motif (italics) was prepared by solid-phase synthesis using the Fmoc strategy on TentaGel RAM resin. Peptides were synthesized using a fully automated Liberty 1 microwave-assisted synthesizer (CEM, Matthews, NC, USA). Peptide cleavage was achieved with a mixture of 90% trifluoroacetic acid (TFA), 5% thioanisole, 3% anisole, and 2% 1,2-EDT over 1.5 h, followed by precipitation in cold diethyl ether. Crude peptide pellets were collected by centrifugation. Peptides were purified by HPLC (Dionex Ultimate 3000; Sunnyvale, CA, USA) using a semipreparative Gemini-NX C18 column (Phenomenex, Torrance, CA, USA) with a gradient of acetonitrile containing 0.1% TFA in water with 0.1% TFA and later lyophilized. The purified peptide was identified by electrospray ionization-mass spectrometry using API 2000 (Thermo Fisher Scientific, Waltham, MA, USA) instrument. Calculated and experimental monoisotopic mass $[M+H]^+$ was 3386.6 and 3387.1, respectively. Before use, the peptide was dissolved in *N*,*N*-dimethylformamide.

Synthesis of biarsenical probes

FlAsH-EDT_2, F2FlAsH-EDT_2, F4FlAsH-EDT_2, Cl2FlAsH-EDT_2, and Cl4FlAsH-EDT_2 were synthesized and purified according to the published protocols (14, 16, 23, 24). Identification was carried out by electrospray ionization-mass spectrometry (ESI-MS; ABI 2000; Thermo Fisher Scientific). The monoisotopic mass values calculated (found) for $[M-H]^-$ were as follows: FlAsH-EDT_2 662.8 (663.1), F2FlAsH-EDT_2 698.8 (699.2), Cl2FlAsH-EDT_2 730.8 (730.9), F4FlAsH-EDT_2 734.8 (735.3), and Cl4FlAsH-EDT_2 798.7 (798.9). Before use, the biarsenical probes were dissolved in anhydrous DMSO. F2FlAsH-EDT_2 and Cl2FlAsH-EDT_2 solutions were prepared fresh because long-term storage in DMSO solution causes probe degradation (16).

Measurement of binding kinetics of biarsenical probes

Fluorescence was recorded on a FluoroMax-4 spectrofluorometer (Horiba Scientific, Irvine, CA, USA). The measurements at pH 7.4 were performed in 50 mM HEPES-Na^+ buffer with 100 mM NaCl and 200 μM *tris*(2-carboxyethyl)phosphine hydrochloride (TCEP). To mimic the lysosomal conditions, we used 20 mM citric buffer with 200 μM TCEP (pH 4.5+). To a series of 3 cuvettes containing the appropriate buffer, and the biarsenical probe was added to a final concentration of 3 μM. The initial fluorescence of the sample was measured, and the $GALA^{412–429}$TC peptide was added to a final concentration of 1 μM. The samples were excited at maximum absorption and fluorescence wavelengths, specific for each biarsenical probe-peptide complex: FlAsH, 509/530 nm; F2FlAsH 510/530 nm; F4FlAsH 528/545 nm; Cl2FlAsH 519/539 nm; and Cl4FlAsH, 530/546 nm. The cuvette holder was set to

37°C. After the measurement, the cuvettes were placed in an incubator set to 37°C with 120 rpm shaking (EcoTron, Infors, Bottmingen-Basel, Switzerland). The fluorescence of the samples was measured at various time points for 10 s for pH 7.4 or 60 s for pH 4.5, and, based on the measurement, the average fluorescence intensity was calculated. Overall, the fluorescence of the samples at pH 7.4 were monitored for 2 h, whereas samples at pH 4.5 were monitored for only 30 min because of precipitation. To test whether the signal increase at pH 4.5 does not come from the biarsenical probe degradation to monoarsenical form, for which florescence is not quenched, the same experiments were performed at pH 4.5 in the absence of the $GALA^{412–429}$ TC peptide. The obtained data points were fitted into single exponential increase function in Origin 8.6 (OriginLab, Northampton, MA, USA). The data for the biarsenical probes at pH 4.5, except F2FlAsH, could not be fitted using this function because of low convergence.

To assess the strength and specificity of the binding the solutions, $GALA^{412–429}$TC-biarsenical probe complexes obtained in the experiment at pH 7.4 were acidified to pH 4.5 by addition of 1 M HCl. Next, the sample was placed in spectrofluorometer and incubated for 5 min at 37°C. The measurement was performed as described above. The sample in the cuvette was stirred at 150 rpm using a magnetic bar. After 1 min since the start of the measurement, EDT solution in DMSO was added to a final concentration of 2.5 mM. The volume of added DMSO was <0.25% of sample volume. The decrease in fluorescence was observed for 20 min. All of the above-mentioned experiments were performed in triplicate.

Plasmid design

For simultaneous expression of LAMP2-red fluorescent protein (RFP) and GALA-TC, we used a bidirectional Tet-On 3G inducible expression system (Takara Bio Europe, Saint-Germain-en-Laye, France). *GLA* cDNA (NM_000169.2) was obtained from pcDNA3.1/GALA cloned into the *Bam*HI and *Bst*BI sites of pcDNA3.1/V5-His to enable for GALA-V5-His expression. Single-stranded DNA oligos encoding the TC-tag (forward: 5′-CGAATTTCTTAATTGTTGCCCGGGCTGCTGTATGGAGCCTTAATT-3′; reverse: 5′-CGAATTAAGGCTCCATACAGCAGCCCGGGCAACAATTAAGAAATT-3′) were annealed, phosphorylated and ligated 3′ to the *Bst*BI site of pcDNA3.1/*GLA*. Sequencing analysis identified the correct orientation of the tag. GALA-TC was PCR-amplified (forward: 5′-CTTTGCGGCCGCATGCAGCTGAGGAACCCAGA-3′; reverse: 5′-CTTTGCGGCCGCTTAAGGCTCCATACAGCAGC-3′) and inserted into the *Not*I site of MCS1 of pTRE3G-BI, to obtain pTRE3G-BI/GALA-TC.

To create LAMP2-RFP, a cDNA clone containing transcript variant LAMP2A (NM_002294.2) was purchased from Source Bioscience (Berlin, Germany). PCR amplification was used to insert 5′-*Bam*HI and 3′-*Xho*I sites and delete the stop codon for the fusion with RFP (forward: 5′-CTTTGGATCCATGGTGTGCTTCCGCCTCTTCC-3′; reverse: 5′-CTTTCTCGAGCCACCACCTCCCAGAGTCTGATATCC-3′). The amplification product was inserted into pCRII-TOPO (Thermo Fisher Scientific) according to the manufacturer's protocol. RFP was amplified from pCAG-DsRed (Addgene, Cambridge, MA, USA) using primers 5′-CTTTCTCGAGCATGGCCTCCTCCGAGAACGTCA-3′ and 5′-CTTTTTCGAACTACAGGAACAGGTGGTGGCGGCC-3′ which added 5′ *Xho*I and 3′ *Bst*BI sites. The PCR product was inserted into pCRII-TOPO vector. Both pCRII-TOPO/LAMP2 and pCRII-TOPO/RFP were digested with *Xho*I which resulted in excised LAMP2 and opened pCRII-TOPO/RFP plasmid. After ligation a PCR was performed (forward: 5′-CTTTCCCGGGATGGTGTGCTTCCGCCTCTT-3′; reverse: 5′-CTTTGGTACCCTACAGGAACAGGTGGTGGC-3′) and *Sma*I (5′) and *Kpn*I (3′) sites were used to insert full-length LAMP2-RFP into MCS2 of pTRE3G-BI/GALA-TC to obtain pTRE3G-BI/GALA-TC:LAMP2-RFP. To obtain pTRE3G-BI/gala[R301Q]-TC:LAMP2-RFP containing mutant GALA, mutagenesis PCR was performed as described elsewhere (21). As a cell culture control pTRE3G-BI/LAMP2-RFP was used that did not contain GALA-TC.

Cell culture and transfection

COS-7 cells were maintained in high-glucose DMEM (Thermo Fisher Scientific) supplemented with pyruvate, L-glutamine, penicillin/streptomycin, and 10% fetal bovine serum (Lonza, Cologne, Germany) in standard cell culture conditions (5% CO_2, 37°C). Before the experiment, the cells were cultivated to obtain 80–90% confluence at the day of transfection. The cells were transfected with a mixture of the respective plasmid constructs (*e.g.*, pTRE3G-BI/LAMP2-RFP or pTRE3G-BI/GALA-TC:LAMP2-RFP and pCMV/Tet3G to induce gene expression with 100 ng/μl doxycycline (Dox) for the LCI experiments) using XFect reagent according to the manufacturer's handbook (Takara Bio Europe).

GALA activity measurement

COS-7 cells were cultured to 80–90% confluence in 24-well plates, transfected with the respective pTRE3G-BI plasmid construct and pCMV/Tet3G using XFect reagent and Dox was added where intended. After 48 h the cells were harvested in deionized H_2O (Labostar, Siemens, Erlangen, Germany). The cells were homogenized by repeated freezing and thawing. After the determination of protein concentration, 0.5 μg of the GALA-TC containing total protein was applied for each measurement, as described elsewhere (21).

Western blot analysis

The COS-7 cells were harvested in RIPA buffer. After the determination of protein concentration, 25 μg of total protein was either digested with endoglycosidase H (Endo H) or peptide-*N*-glycosidase F (both obtained from NEB, Frankfurt am Main, Germany) or directly subjected to SDS-PAGE. Detection of GALA-TC was performed with mouse monoclonal anti-GALA antibody (ab169315; Abcam Inc, Cambridge, United Kingdom) at a dilution of 1:1,000 in Tris-buffered saline, 0.1% Tween and 3% skim dry milk for 1 h. Mouse monoclonal anti-GAPDH antibody (ab8245) at a 1:10,000 dilution was used as a loading control. Secondary antibodies goat antimouse IRdye800CW and goat antimouse IRdye680LT were used for visualization using an Odyssey Infrared Imager (Li-Cor Biosciences, Lincoln, NE, USA).

Live cell imaging

Labeling

After transfection of 80–90% confluently grown COS-7 cells and addition of Dox for 24 h, the cells were trypsinized and transferred onto poly-D-lysine-coated chambered cover glasses (Chambered Coverglass, 4 Wells; Nunc Lab-Tek, Roskilde, Denmark) at a density of $4.5 \times 10^4/cm^2$ and cultivated for another 24 h in the presence of Dox to ensure monolayer growth for optimal microscopic results. For every labeling condition the cells were seeded in duplicate chambers.

The labeling protocol was modified from Hoffmann *et al.* (25). Before labeling, the cells were either pretreated with 1 mM TBP or the respective solvent DMSO for 15 min, followed by a change of

medium (DMEM, high glucose, and 25 mM HEPES, without phenol red). This labeling medium contained the indicated biarsenical probe at a final concentration of 1 mM. Samples were incubated at 5% CO_2 and 37°C for 3 h. After labeling, cells were washed with 2.5 mM EDT for 10 min to remove excess probe. During the imaging process, they were kept in imaging buffer (pH 7.3; 140 mM NaCl, 5.4 mM KCl, 2 mM $CaCl_2$, 1 mM $MgCl_2$, and 10 mM HEPES) as suggested by Hoffmann *et al.*

Image acquisition

Final visualization was achieved with the BZ-800 microscope system (Keyence, Neu-Isenburg, Germany) using a PlanApo 40X/NA0.95 objective (Nikon, Tokyo, Japan). First, transfected cells were identified by the Lamp2-RFP signal. For detection, the TexasRed filter cube was used with the following specifications: excitation filter (EX) 560/40, dichroic mirror (DM) 595, and barrier filter (BA) 630/60. Exposure time was 2000 ms. GALA-TC was detected with FlAsH-EDT_2 or its analogs with a YFP filter cube with the following specifications: EX, 500/20 nm; DM, 515 nm; and BA 515/30 nm and exposure time was 250 ms. Exposure time for the detection of DAPI was 100 ms. The DAPI-B filter cube was used with the following specifications: EX, 360/40; DM, 400; and BA, 460/50 (all filter cubes from Keyence).

Imaging data analysis

Fiji software (26) was used for the image analysis. The red channel image shows Lamp2-RFP positive signal indicating lysosomal areas. A pixel signal intensity ranging from 91/255 to 255/255 was considered RFP positive and selected as the region of interest (ROI). The ROI was transferred to the green channel image, and the green fluorescence intensity was measured inside selected areas (range, 0–255 per pixel). Baseline signal intensity was determined with the mean signal intensity of control vector (pTRE3G-BI/LAMP2-RFP) transfected cells. The pictures were automatically analyzed using an adapted script. ImageJ software (National Institutes of Health, Bethesda, MD, USA) analysis was used to transfer the ROI into the corresponding green channel image.

RESULTS

In a first attempt to label GALA-TC in cell culture with a conventional FlAsH-EDT_2 probe, a 1 h labeling protocol led to a very low fluorescence signal (data not shown). We hypothesized that the acidic lysosomal environment (pH 4–5) either did not provide suitable conditions for a proper binding between the FlAsH-EDT_2 probe and GALA-TC or prevented the emission of fluorescence because of the relatively high pK_a of the 3′-hydroxyl group that governs xanthenes-based dyes pH-fluorescence dependence. The pK_a of F1AsH in complex with a TC-tag is 5.4. We selected 4 FlAsH-EDT_2 analogs with lower pK_a in the complex with TC: F2FlAsH-EDT_2 (3.66), F4FlAsH-EDT_2 (4.95), Cl2FlAsH-EDT_2 (3.32), and Cl4FlAsH-EDT_2 (5.02). To investigate the optimal conditions for biarsenical probe-mediated fluorescence-based LCI of a lysosomal enzyme (14, 16). Initial *in vitro* binding and stability studies were performed at pH 7.4 and 4.5 to mimic the environment of the cytoplasm or ERER, the cellular site of folding, processing, and sorting proteins and inside lysosomes, respectively.

First, to test usability of the TC tag system at acidic pH we established an *in vitro* binding assay. Expression of GALA in *E. coli* results in inactive and truncated protein (27) and, thus, GALA protein fused with C-terminal TC tag would require a mammalian expression system to obtain its complex glycosylation state and correct conformation, we decided against the use of a fully recombinant GALA-TC. For convenience a readily available peptide model was used which that proved efficient to characterize biarsenical probe binding *in vitro* (25, 28).

A model target containing the octadecapeptide representing the C-terminal sequence of GALA was synthesized with added TC-tag sequence. The peptide was prepared in such a way to represent the tag position in full protein used in later cell culture–labeling experiments. The resulting peptide (NH_2-TVLLQLENTMQMSLKDLL*FLNCCPGCCMEP*-amide, $GALA^{412–429}TC$) was used for *in vitro* binding assays of FlAsH-EDT_2 and the 4 derivatives. At pH 7.4, enhanced fluorescence signal was detected for all used biarsenical probes indicating the proper binding of the fluorophores to $GALA^{412–429}TC$ (**Fig. 1*A***). The F2FlAsH-$GALA^{412–429}TC$ complex had larger fluorescence and the probe-binding kinetics were more rapid compared to the other probes. Binding rates changed at the lower pH of 4.5. FlAsH and Cl2FlAsH labels exhibited poor, yet measurable fluorescence increase despite the low pK_a of the latter probe. The F2FlAsH-$GALA^{412–429}TC$ complex exhibited the highest fluorescence in comparison to the complexes with other biarsenical probes at this pH (Fig. 1*B*). F4FlAsH- and Cl4FlAsH-TC complexes also significantly increased their fluorescence; however, the overall fluorescence intensity was much lower than for F2FlAsH- $GALA^{412–429}TC$ complex.

Because the fluorescence of monoarsenical species is not efficiently quenched compared to the biarsenical form, it is unlikely that the increase in fluorescence was related to biarsenical probe decomposition. The incubation of all biarsenical probes in pH 4.5 buffer without tetracysteine peptide showed no significant increase in fluorescence over the time of the experiment. It should be noted that all experiments at pH 4.5 were performed for 30 min, as longer incubation times resulted in precipitate formation. The lower signal intensity probably stems from lower reaction rate at acidic pH. Based on the shape of the F2FlAsH/$GALA^{412–429}TC$ binding curve that showed a plateau after 30 min, we first assumed that all peptide was bound to the probe, but it is more likely that 30 min represents the point at which the increase in fluorescence is overruled by the loss of signal due to precipitation. We observed rapid signal loss at longer incubation times (data not shown). Analysis of the binding kinetics also revealed lower reaction rates at acidic pH. The results herein suggest that a longer incubation with the probe in the cell culture experiment may be helpful to obtain best signal-to-noise ratio. Moreover, it has been suggested that an increase in EDT concentration during cell washing can also improve the signal quality. Addition of EDT to the solution *in vitro* also provides information about the biarsenical probe-TC complex stability. We therefore tested the complex stability at pH 4.5 in the presence of 2.5 mM EDT. To do so, samples containing $GALA^{412–429}TC$ and biarsenical probe were incubated at pH 7.4 for 2.5 h. On the basis of previous experiments, it was assumed that, at this late time point, all peptide was bound to the biarsenical probe (see Fig. 1*A*, plateau phase). Then, the pH was adjusted to 4.5 and EDT was added to a final concentration of 2.5 mM. After 20 min, the fluorescence decreased significantly. However, the percentage of the final fluorescence signal compared to the initial values was above 65% in all cases (**Table 1**). Cl4FlAsH-, Cl2FlAsH- and F2FlAsH-$GALA^{412–429}TC$ complexes retained higher fluorescence than the FlAsH-$GALA^{412–429}TC$ complex, which evidences a higher stability under the conditions used. It should be noted that the fluorescence of the complexes was immediately lowered after acidification. However, the data suggest that this decrease in fluorescence stemmed only from the pK_a of the biarsenical probe and not from precipitation. In all cases, the fluorescence was significantly higher than in the $GALA^{412–429}TC$-binding experiments in which acidic conditions were used from the start, which

COLOR

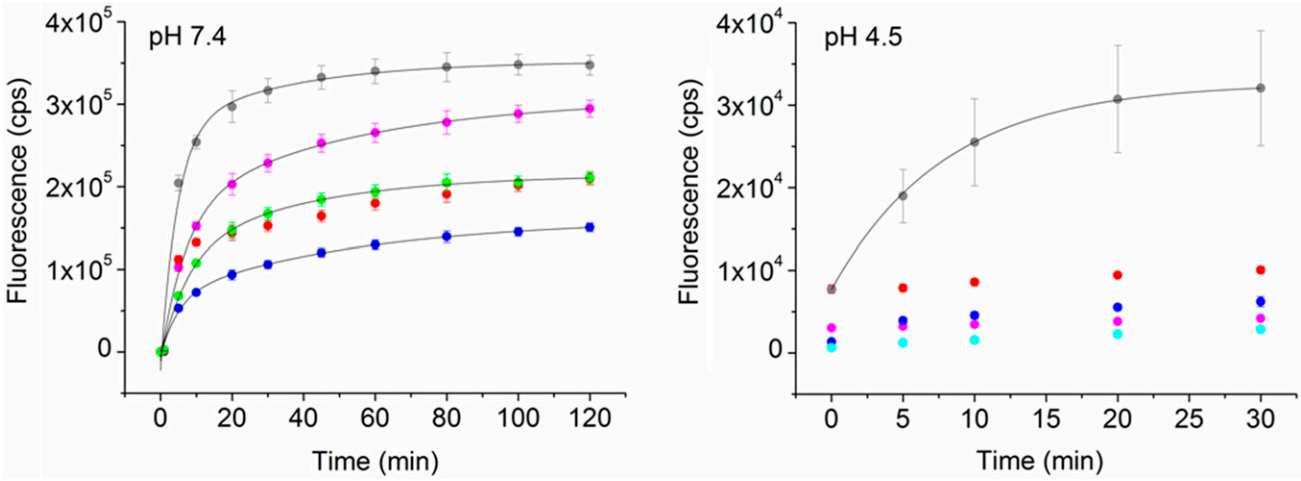

Figure 1. Increase of fluorescence signal from various biarsenical probes upon incubation with GALA$^{412–429}$TC peptide at pH 7.4 (*A*) and 4.5 (*B*). The filled signs represent data points for the complex of the GALA$^{412–429}$TC peptide labeled with FlAsH (pink), Cl2FlAsH (red), F2FlAsH (gray), Cl4FlAsH (blue), or F4FlAsH (green) fluorophores. *A*) At pH 7.4 all of the biarsenical probes efficiently bind to the GALA$^{412–429}$TC, forming a fluorescence complex. After 120 min of recording, a plateau of the fluorescence signals was attained for all probes tested, and the measurement was stopped. *B*) At lower pH, only F2FlAsH efficiently formed a highly fluorescent complex with GALA$^{412–429}$TC, albeit at a slower rate compared with pH 7.4. Close inspection of the data revealed that F4- and Cl4FlAsH also significantly increased their fluorescence, but the overall fluorescence of the complex was not significant. The experiments were performed using 1 μM GALA$^{412–429}$TC and 3 μM biarsenical probe at 37°C. The data are means ± SD of at least 3 independent experiments.

supports our previous conclusion that the formation of the fluorescent complex is much slower at lower pH.

In light of our *in vitro* findings, we designed a specified protocol for the LCI approach modified from Hoffmann and colleagues (25) by 1) elongating the labeling phase to 3 h; 2) using the membrane-permeable reducing agent TBP, considering the relative oxidizing redox status within the Golgi apparatus and lysosomes (29, 30); and 3) increasing the EDT concentration to 2.5 mM for the washing step, yielding an enhanced signal-to-noise ratio (data not shown; see also Ref. 31). Conventional FlAsH-TC labeling was used to establish a robust workflow (**Fig. 2**). In detail, lysosomal compartments in pTRE3G-BI/GALA-TC:LAMP2-RFP and control vector pTRE3G-BI/LAMP2-RFP transfected COS-7 cells were identified by positive Lamp2-RFP signal (Fig. 2*A1*, *B1*). With that, the GALA-TC/FlAsH complex-emitted green fluorescence signal was measured in these areas (Fig. 2*A3*, *B3*). Optimal analysis parameters were defined. To obtain highest sensitivity of the protocol, data were normalized by dividing GALA-TC:LAMP2-RFP fluorescence by control vector transfected cells, thereby ascertaining fold change analysis and enabling for a comparison of the different probes. It should be noted that we determined correct localization of Lamp2-RFP with a counterstain against endogenous LAMP2 to prove colocalization of the signals (Supplemental Fig. 2).

Thus far, there have been no reports of GALA fusion proteins that are suitable for LCI. Only 1 report has described a GALA fusion protein that uses the transduction domain of HIV-derived TAT protein, a very small epitope tag. This fusion construct, however, requires the use of antibodies for imaging and is thus not suitable for LCI. No functional constraint was reported for this construct by Higuchi and colleagues (32), but both intracellular processing and the activity of *in situ*-expressed enzyme have not been analyzed. In an earlier, unpublished study we observed a significant enzyme activity reduction of C-terminal V5-His$_6$ fusion protein (pcDNA3.1 vector). *Ex vivo* enzyme activity in HEK293H cells episomally expressing the GALA-V5 construct decreased to 62.7% compared to the native enzyme. No apparent reduction of enzyme activity was observed using hemagglutinin-derived or DYKDDDDK (FLAG) tags (pCMV-HA-C, pCMV-DYKDDDDK-C vectors). A fusion construct with GFP entirely prevented protein synthesis, which is suggested by the absence of GALA-GFP signal in both Western blot and fluorescence microscopy (Supplemental Fig. 3). To generate functional lysosomal TC-tagged GALA fusion protein that allowed for fluorescence detection in living cells, we tested several TC-tag variants for enzyme performance. SFEEAAAR-EACCRECCARA (33) and SFERTGAGGCCPGCCGGG yielded strongly reduced enzyme activity compared to the native wild-type enzyme and were consequently excluded. An optimized tag sequence (FLNCCPGCCMEP) was selected for the study, because it yielded the highest *ex vivo* enzyme activity of 76.9%.

The pTRE3G-BI/GALA-TC:LAMP2-RFP construct expresses active GALA enzyme that carries the FLNCCPGCCMEP sequence. Intracellular GALA-TC level and activity were elevated in a Dox dose-dependent manner (**Fig. 3*A***) and GALA was detected as a mature protein of ~46 kDa (Fig. 3*B*). When compared to overexpressed native GALA, GALA-TC shows a distinct band that displays a shift that corresponds to the calculated molecular weight of the linker and TC tag (1.68 kDa). GALA-TC and native GALA were equivalently processed by COS-7 cells as further demonstrated by the removal of N-linked glycosides. TC-tagged mutant GALA [gala(R301Q)-TC], however, shows several bands in the Western blot, which is indicative of the different cellular

TABLE 1. *Percentage of initial fluorescence signal emitted by the biarsenical probe-GALA$^{412–429}$TC complex at pH 4.5, 20 min after addition of 2.5 mM EDT*

Complex	Initial fluorescence (%)
FlAsH- GALA$^{412–429}$TC	72 ± 2
Cl2FlAsH- GALA$^{412–429}$TC	82 ± 4
F2FlAsH- GALA$^{412–429}$TC	80 ± 4
Cl4FlAsH- GALA$^{412–429}$TC	102 ± 8
F4FlAsH- GALA$^{412–429}$TC	68 ± 2

n = 3. Data are mean percentages ± SD.

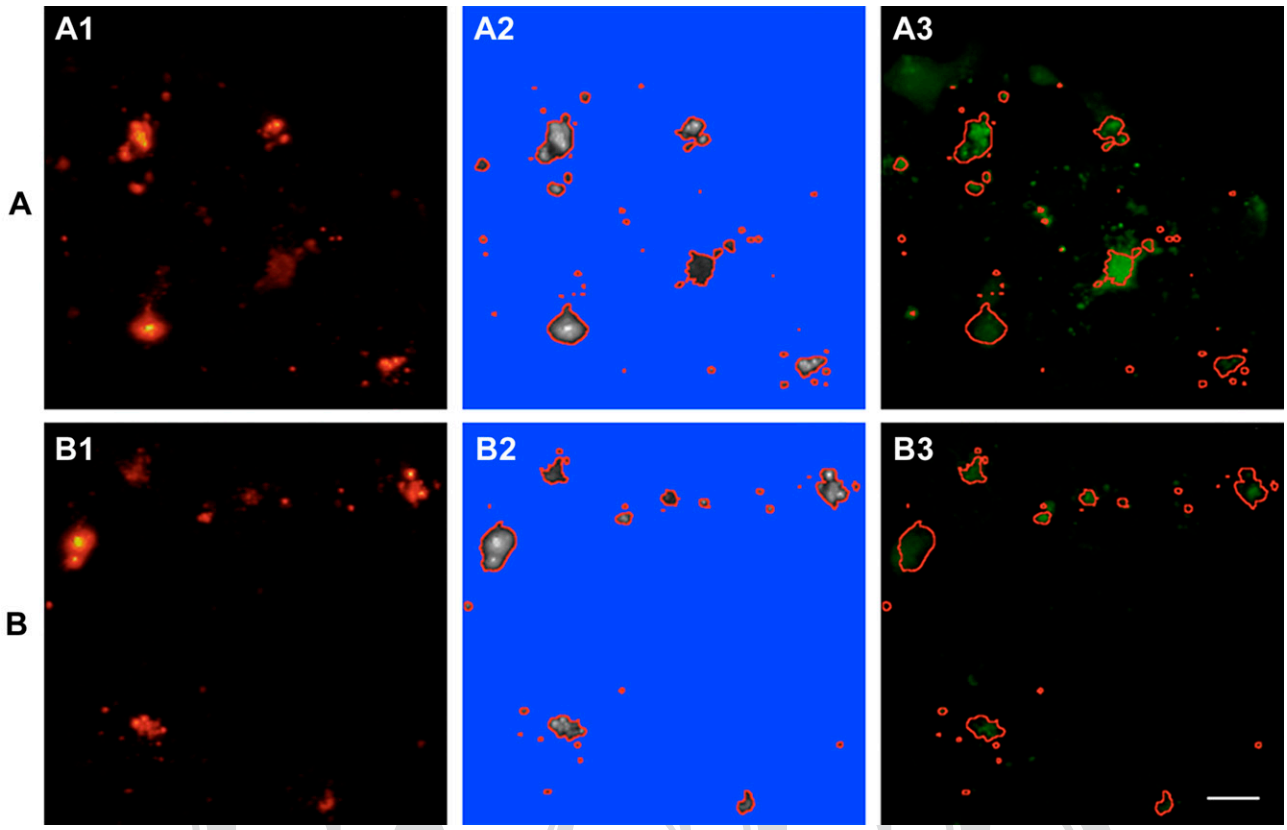

COLOR

Figure 2. Quantitative computational analysis of COS-7 cells expressing GALA-TC. *A*) After transfection of COS-7 cells with pTRE3G-BI/GALA-TC:LAMP2-RFP and labeling with FlAsH-EDT$_2$ for 3 h [a protocol containing 6 h labeling has also been tested resulting in increased cell death and, consequently, poorer fluorescence (data not shown)], the image was first examined in the red channel (*A1*) to set a stringent threshold (91/255) and select the lysosomal area by ImageJ's Create Selection function (*A2*). The selection was saved in the ROI manager and transferred to the green channel, to measure FlAsH fluorescence signal within lysosomal compartments only (*A3*). *B*) In contrast to *A*, COS-7 cells were transfected with pTRE3G-BI/LAMP2-RFP control vector (*B1-B3*). This strategy was followed to determine unspecific background signal. Scale bar, 10 μm.

fractions where mutant enzyme is present. Moreover, the migration behavior after Endo H- and PNGase F–mediated deglycosylation was distinct from that of GALA and GALA-TC. The presence of the double band reflects the presence of immature GALA enzyme that was not ultimately processed.

Unexpectedly, we were unable to detect an Endo H resistant GALA fraction. Endo H was able to fully deglycosylate both GALA and GALA-TC, which is indicative of a negligible fraction of intracellular human recombinant GALA that carried complex sugar chains compared to a large fraction that carried the high-mannose glycosylation type (34). A similar result of the deglycosylation reaction was obtained for endogenous GALA in the COS-7 cells (data not shown). Based on these results, we concluded that pTRE3G-BI/GALA-TC:LAMP2-RFP expresses fully functional GALA enzyme and was evidently viable for the lysosomal localization study.

Figure 3C shows the quantitative analysis for the 5 biarsenical probes. The median of the fold-change was >1 for all analyzed compounds. Without using TBP all probes showed similar results without a significant improvement to the conventional FlAsH-EDT$_2$. However, use of TBP made it evident that FlAsH-EDT$_2$ did poorly in comparison with its analogs, which is in accord with our preliminary findings. Labeling with Cl4FlAsH-EDT$_2$ and F4FlAsH-EDT$_2$ did not significantly improve the signal-to-noise ratio as expected, based on the *in vitro* results. Both Cl2FlAsH and F2FlAsH complexes showed overall improved fluorescence. Figure 3*D* depicts a typical result for FlAsH-EDT$_2$ and F2FlAsH-EDT$_2$. The corresponding data points are highlighted in blue (Fig. 3C). The bottom panels indicate diffuse fluorescence signal of a typical control vector–transfected specimen compared to specific lysosomal localization of fluorescence in GALA-TC transfected cells.

To determine whether mutant GALA enzyme displays a trafficking deficit that results in its mislocalization, we stained COS-7 cells expressing gala(R301Q)-TC and compared the mutant with wild-type GALA (**Fig. 4**). F2FlAsH-EDT$_2$ probe labeling was effective in revealing different cellular localization of the 2 enzymes. A 7.9-fold stronger colocalization was detected for GALA-TC compared to the mutant enzyme, which was barely found in lysosomes, as shown by the lysosomal visualization using LAMP2-RFP. As other studies have indicated, it is highly likely that the gala(R301Q)-TC is localized to the ER (18, 35).

DISCUSSION

The purpose of this project was to establish a protocol for the detection of a medium-sized soluble enzyme in a cellular compartment that has been traditionally difficult with the LCI approach. GALA is an intraluminal lysosomal glycosidase. It breaks down complex macromolecules, such as globotriaosylceramide. GALA deficiency causes the human metabolic Anderson-Fabry disease. The functional holoenzyme consists of 2 monomeric GALA units. The C-terminal end of the protein is free for a peptide tag fusion (36).

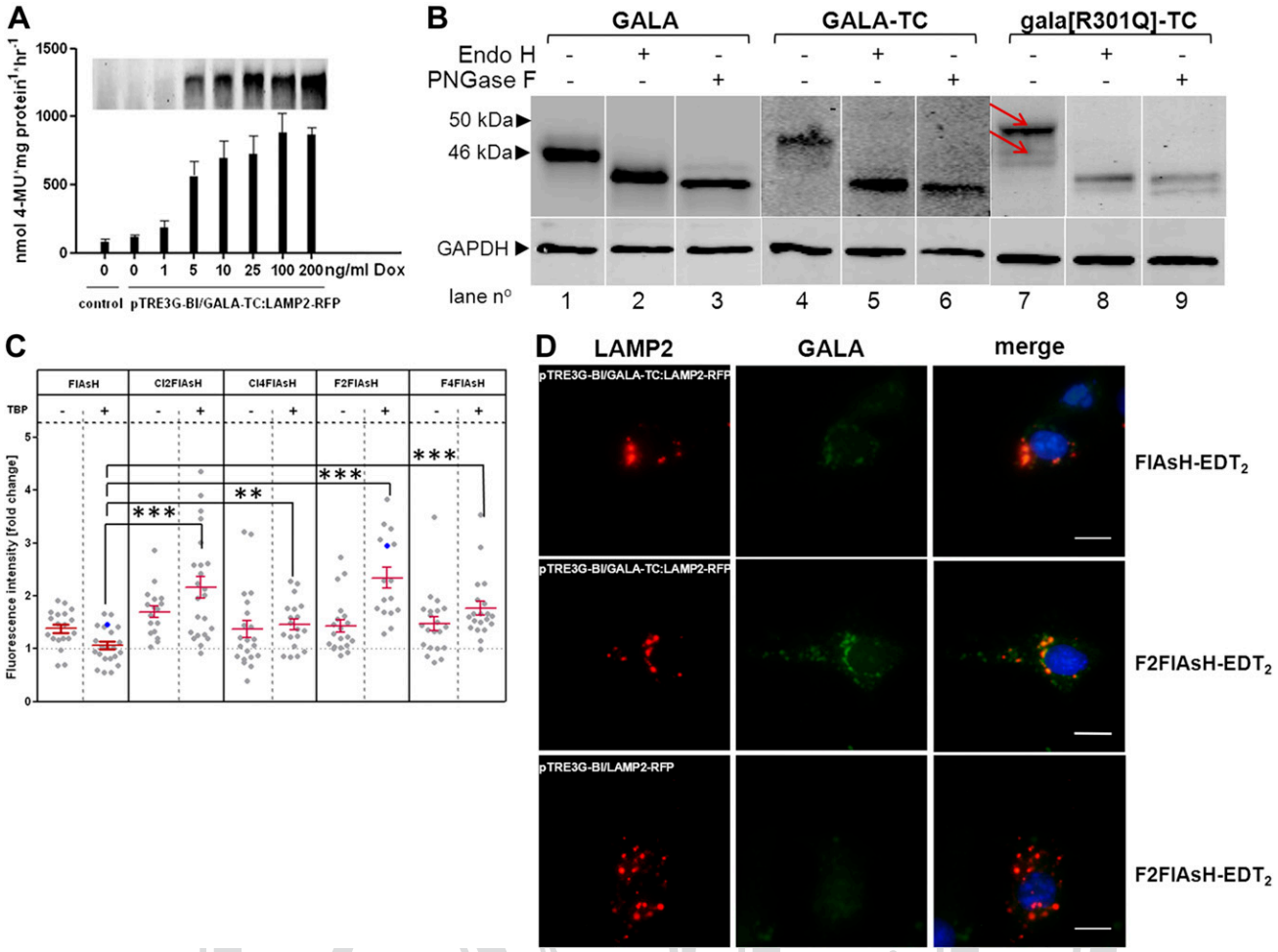

COLOR

Figure 3. Biochemical characterization and LCI of TC-tagged GALA enzyme. *A*) pTRE3G/GALA-TC:LAMP2-RFP-transfected COS-7 cells were treated with increasing concentrations of Dox to induce GALA-TC and LAMP2 expression from a bidirectional promoter. GALA-TC activity and protein content of the cells was found to be elevated in a concentration-dependent manner 48 h after transfection. Data were obtained from 3 independent experiments and are means ± SD. *B*) Similarly, GALA-TC of pTRE3G/GALA-TC:LAMP2-RFP-transfected COS-7 cells was subjected to band shift analysis with untreated and EndoH/PNGaseF-treated lysates in comparison to wild-type and mutant GALA (gala[R301Q]-TC). Untagged wild-type GALA presented as a single band (lane 1) with a band size of ~46 kDa. GALA-TC presented a single band (lane 4) of ~48 kDa, reflecting the size of the protein increased by the TC tag. Mutant GALA displayed several bands, indicating different/incomplete intracellular processing. Red arrows: mature lysosomal (~46 kDa) and immature ER form (~50 kDa). Deglycosylation analysis revealed similar digestion patterns for GALA and GALA-TC as well, whereas the mutant enzyme showed the presence of a strong additional band. *C*) Normalized intracellular signal intensity of biarsenical probe/GALA-TC complex–emitted fluorescence of pTRE3G/GALA-TC:LAMP2-RFP-transfected COS-7 cells. Data are shown as fold change relative to the value of control vector transfected cells, whose mean fluorescence was obtained by normalization of 10 randomly selected image sections from each parallel experiment. An unpaired 2-tailed Student's *t* test was performed for the TBP-treated experimental series. $*P > 0.05$; $**P > 0.01$; $***P > 0.005$, performances of FlAsH-EDT$_2$ *vs.* those of the analogs. *D*) FlAsH-EDT$_2$- and F2FlAsH-EDT$_2$-labeled COS-7 cells transfected with either pTRE3G-BI/GALA-TC:LAMP2-RFP (top and middle panels) or control vector (bottom panel). Data points obtained from the FlAsH-EDT$_2$ and F2FlAsH-EDT$_2$ staining are highlighted in blue in *C*. Scale bars, 10 μm.

We observed a poor signal-to-noise ratio when using commercially available FlAsH-EDT$_2$ to detect C-terminal TC-tagged GALA. Because this probe was not amenable for use in lysosomal localization studies, we sought to identify a novel probe that provided favorable binding kinetics and yielded improved signal-to-noise ratio under oxidative and acidic conditions. Because the initial analysis suggested that the pK_a of 5.4 for the FlAsH-TC complex is too high to provide strong fluorescence signal in lysosomes, we turned to chlorine and fluorine analogs. The pK_a is significantly decreased for Cl2FlAsH- and F2FlAsH-complex because of induction effect from halogen atoms at positions 2′ and 7′. *In vitro* recordings showed improved fluorescent signal of F2FlAsH-EDT$_2$, F4FlAsH-EDT$_2$, and Cl4FlAsH-EDT$_2$ upon incubation with GALA$^{412–429}$TC peptide under acidic conditions that resemble the lysosomal environment (Fig. 1*B*), with the first one having the highest fluorescence intensity. At pH 7.4 the signal intensity and kinetics of the FlAsH-EDT$_2$ analogs was in a comparable range (Fig. 1*A*).

For the protein labeling experiments, COS-7 cells were used to coexpressed LAMP2-RFP and GALA-TC from a

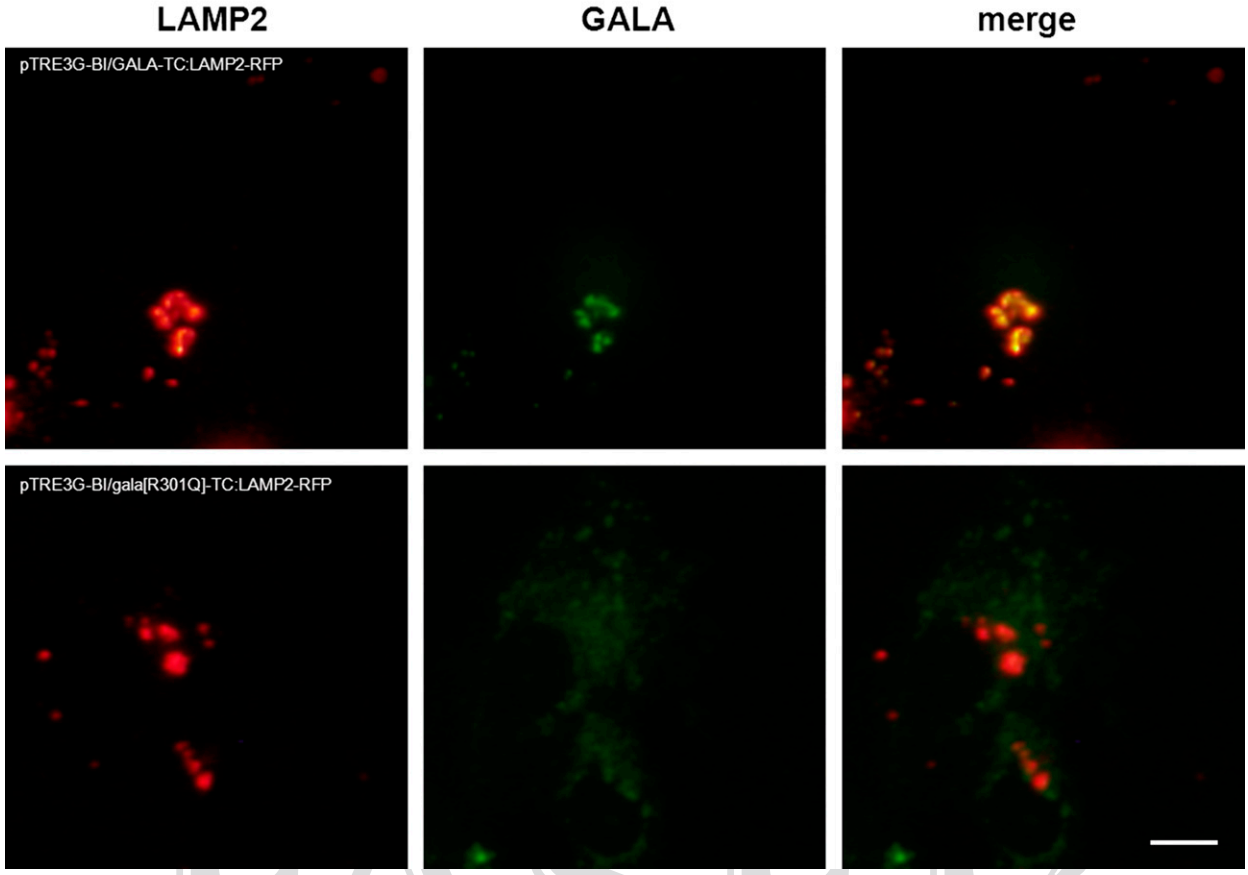

COLOR

Figure 4. Disease-related mutant GALA mislocation in COS-7 cells. Mutant gala[R301Q]-TC was over-expressed in COS-7 and compared to the wild-type enzyme. Cells were treated with TBP and labeled with F2FlAsH-EDT_2 for 3 h, according to the optimized protocol. Top panel: gala[R301Q]-TC. A rather diffuse F2FlAsH signal is suggestive of a scattered distribution of this mutant. There is limited colocalization with LAMP2-RFP indicating that most gala[R301Q]-TC is localized outside of the lysosomes. Bottom panel: wild-type GALA-TC. The enzyme is represented as a focal signal that is mainly colocalized with the LAMP2-RFP signal, indicating that a predominant fraction of GALA-TC is situated within the lysosomal fraction of the cell. Scale bar, 10 μm.

bidirectional promotor. Lamp2 protein was fused to the RFP *via* its cytosolic C-terminal part allowing for local determination of lysosomes (Figs. 2 and 3*D*). The different FlAsH-EDT_2 analogs revealed a better resolution of positive GALA-TC signal (Fig. 3*C*). However, only F2FlAsH-EDT_2 and Cl2FlAsH-EDT_2 in combination with TBP were able to visualize GALA-TC significantly better than FlAsH-EDT_2. Even though the *in vitro* binding studies revealed that F4FlAsH-EDT_2 and Cl4FlAsH-EDT_2 significantly increased their fluorescence upon binding to $GALA^{412–429}$TC peptide, the 2 compounds could not be validated as superior in the LCI experiments. Such a result can easily stem from the different *in vitro* and intracellular conditions in terms of the viscosity, presence of proteins, and small chemical molecules, and so forth. The superiority of F2FlAsH-TC stems from the presence of fluorine atoms, which lowers the pK_a. Consequently, the fluorescence at pH 4.5 rests at a comparable level to that measured at pH 7.4. Unfortunately, the use of pH-independent fluorescent probes is precluded by the technical challenge to synthesize biarsenical rhodamines, likely because of steric hindrance. AsCy3-EDT_2, a cyanine biarsenical probe has not been used in cell lines, and the required distance between cysteine residues pairs in the binding motif is still controversial (37). Further enhancement of the xanthene-based probes in terms of lowering the pK_a also seems problematic as Cl6- and F6FlAsH-EDT_2 probes instantly decomposed to monoarsenical species and then to initial substrate (16). In view of this information, it seems that the only way to improve this system is to perform another optimization of the amino acid residues flanking the TC-binding motif specifically on the lysosomal target. Such an optimization could introduce additional interactions between the biarsenical probe and the binding tag, which could increase the dissociation constant of the complex or increase its fluorescence. Such an optimization has been performed on cells to obtain the FLNCCPGCCMEP sequence used in this study (22).

Although we could demonstrate that GALA-TC is processed similarly to its untagged wild-type counterpart, a rather large fraction of GALA-TC was detected in the extralysosomal areas. This fraction likely reflects the steady-state level of GALA-TC enzyme *en route* to the lysosome. A possible explanation for the high signal abundance and intensity may be provided by the lower binding kinetics as well as the response to the EDT wash *in vitro*,

which can cause significant disturbance of the probe binding under lysosomal conditions *in situ*. Hence, extralysosomal GALA-TC presents a relatively stronger signal because it is more efficiently labeled. Moreover, GALA-TC expression from the inducible pTRE3G-BI promotor was considerably lower than obtained by a conventional cytomegalovirus promotor vector, which may contribute to an overall unfavorable signal-to-noise ratio and presents a technical challenge for automated drug screens. However, we were able to distinguish cellular localization patterns derived from wild-type and mutant enzyme. In an earlier study, it was reported that the cellular steady-state level of disease-related mutant GALA is rather low compared to the wild-type enzyme, because of effective and rapid ERAD (21). This finding further emphasizes that biarsenical FlAsH-EDT_2-derived probes, especially F2FlAsH, provide a robust high-affinity labeling alternative for the detection and quantification of the intralysosomal fraction of lysosomal proteins in LCI.

In summary, we demonstrate the feasibility of using LCI for visualization of a soluble lysosomal enzyme that was unsuitable for conventional labeling using FPs. Imaging of TC-tagged lysosomal GALA protein using the biarsenical probe FlAsH-EDT_2 yielded an improper signal-to-noise ratio. However, the establishment of an appropriate TC-tagged GALA protein and the use of fluorinated F2FlAsH-EDT_2 led to a superior detection and can be recommended for proteins in an acidic cellular environment. The correction of the cellular transport of mutant enzymes is important for therapeutic intervention in AFD and other lysosomal storage disorders. To this end, F2FlAsH-EDT_2 can aid the development of imaging-based systems to analyze subcellular localization of proteins and to screen for effective pharmacologic chaperones. FJ

ACKNOWLEDGMENTS

The authors thank Flora Luo (Harvard Medical School, Boston, MA, USA) for language editing. This work was supported by grants from the University Rostock Medical Center (promotion of young researchers) and the National Science Centre (NCN, Krakow, Poland) under OPUS Grant 2016/21/B/NZ1/02847 (to A.K.). The authors declare no conflicts of interest.

AUTHOR CONTRIBUTIONS

C. Bohl, A. Pomorski, A. Rolfs, and J. Lukas designed the research; C. Bohl, A. Pomorski, S. Seemann, A.-M. Knospe, and J. Lukas performed the research; C. Bohl, A. Pomorski, and J. Lukas analyzed the data; A. Pomorski, A. Krężel, and J. Lukas wrote the paper; and C. Zheng, A. Pomorski, and A. Krężel contributed new reagents or analytic tools.

REFERENCES

1. Soon, L., Braet, F., and Condeelis, J. (2007) Moving in the right direction-nanoimaging in cancer cell motility and metastasis. *Microsc. Res. Tech.* **70**, 252–257
2. Shih, W., and Yamada, S. (2011) Live-cell imaging of migrating cells expressing fluorescently-tagged proteins in a three-dimensional matrix. *J. Vis. Exp.* **58,** 3589
3. Miller, M. J., Safrina, O., Parker, I., and Cahalan, M. D. (2004) Imaging the single cell dynamics of CD4+ T cell activation by dendritic cells in lymph nodes. *J. Exp. Med.* **200**, 847–856
4. Nägerl, U. V., Willig, K. I., Hein, B., Hell, S. W., and Bonhoeffer, T. (2008) Live-cell imaging of dendritic spines by STED microscopy. *Proc. Natl. Acad. Sci. USA* **105**, 18982–18987
5. Ilegems, E., Pick, H. M., Deluz, C., Kellenberger, S., and Vogel, H. (2004) Noninvasive imaging of 5-HT3 receptor trafficking in live cells: from biosynthesis to endocytosis. *J. Biol. Chem.* **279**, 53346–53352
6. Schwarz-Romond, T., Merrifield, C., Nichols, B. J., and Bienz, M. (2005) The Wnt signalling effector Dishevelled forms dynamic protein assemblies rather than stable associations with cytoplasmic vesicles. *J. Cell Sci.* **118**, 5269–5277
7. Wombacher, R., Heidbreder, M., van de Linde, S., Sheetz, M. P., Heilemann, M., Cornish, V. W., and Sauer, M. (2010) Live-cell super-resolution imaging with trimethoprim conjugates. *Nat. Methods* **7**, 717–719
8. Subach, O. M., Gundorov, I. S., Yoshimura, M., Subach, F. V., Zhang, J., Grüenwald, D., Souslova, E. A., Chudakov, D. M., and Verkhusha, V. V. (2008) Conversion of red fluorescent protein into a bright blue probe. *Chem. Biol.* **15**, 1116–1124
9. Stadler, C., Rexhepaj, E., Singan, V. R., Murphy, R. F., Pepperkok, R., Uhlén, M., Simpson, J. C., and Lundberg, E. (2013) Immunofluorescence and fluorescent-protein tagging show high correlation for protein localization in mammalian cells. *Nat. Methods* **10**, 315–323
10. Landgraf, D., Okumus, B., Chien, P., Baker, T. A., and Paulsson, J. (2012) Segregation of molecules at cell division reveals native protein localization. *Nat. Methods* **9**, 480–482
11. Gahlmann, A., and Moerner, W. E. (2014) Exploring bacterial cell biology with single-molecule tracking and super-resolution imaging. *Nat. Rev. Microbiol.* **12**, 9–22
12. Giraldez, T., Hughes, T. E., and Sigworth, F. J. (2005) Generation of functional fluorescent BK channels by random insertion of GFP variants. *J. Gen. Physiol.* **126**, 429–438
13. Fernández-Suárez, M., and Ting, A. Y. (2008) Fluorescent probes for super-resolution imaging in living cells. *Nat. Rev. Mol. Cell Biol.* **9**, 929–943
14. Griffin, B. A., Adams, S. R., and Tsien, R. Y. (1998) Specific covalent labeling of recombinant protein molecules inside live cells. *Science* **281**, 269–272
15. Pomorski, A., and Krężel, A. (2011) Exploration of biarsenical chemistry–challenges in protein research. *ChemBioChem* **12**, 1152–1167
16. Pomorski, A., Adamczyk, J., Bishop, A. C., and Krężel, A. (2015) Probing the target-specific inhibition of sensitized protein tyrosine phosphatases with biarsenical probes. *Org. Biomol. Chem.* **13**, 1395–1403
17. Golubev, A. M., Nagem, R. A. P., Brandão Neto, J. R., Neustroev, K. N., Eneyskaya, E. V., Kulminskaya, A. A., Shabalin, K. A., Savel'ev, A. N., and Polikarpov, I. (2004) Crystal structure of α-galactosidase from Trichoderma reesei and its complex with galactose: implications for catalytic mechanism. *J. Mol. Biol.* **339**, 413–422
18. Ishii, S., Chang, H. H., Kawasaki, K., Yasuda, K., Wu, H. L., Garman, S. C., and Fan, J. Q. (2007) Mutant alpha-galactosidase A enzymes identified in Fabry disease patients with residual enzyme activity: biochemical characterization and restoration of normal intracellular processing by 1-deoxygalactonojirimycin. *Biochem. J.* **406**, 285–295
19. Park, J. Y., Kim, G. H., Kim, S. S., Ko, J. M., Lee, J. J., and Yoo, H. W. (2009) Effects of a chemical chaperone on genetic mutations in α-galactosidase A in Korean patients with Fabry disease. *Exp. Mol. Med.* **41**, 1–7
20. Filoni, C., Caciotti, A., Carraresi, L., Cavicchi, C., Parini, R., Antuzzi, D., Zampetti, A., Feriozzi, S., Poisetti, P., Garman, S. C., Guerrini, R., Zammarchi, E., Donati, M. A., and Morrone, A. (2010) Functional studies of new GLA gene mutations leading to conformational Fabry disease. *Biochim. Biophys. Acta* **1802**, 247–252
21. Lukas, J., Giese, A. K., Markoff, A., Grittner, U., Kolodny, E., Mascher, H., Lackner, K. J., Meyer, W., Wree, P., Saviouk, V., and Rolfs, A. (2013) Functional characterisation of alpha-galactosidase a mutations as a basis for a new classification system in fabry disease. *PLoS Genet.* **9**, e1003632
22. Martin, B. R., Giepmans, B. N., Adams, S. R., and Tsien, R. Y. (2005) Mammalian cell-based optimization of the biarsenical-binding

tetracysteine motif for improved fluorescence and affinity. *Nat. Biotechnol.* **23**, 1308–1314
23. Spagnuolo, C. C., Vermeij, R. J., and Jares-Erijman, E. A. (2006) Improved photostable FRET-competent biarsenical-tetracysteine probes based on fluorinated fluoresceins. *J. Am. Chem. Soc.* **128**, 12040–12041
24. Pomorski, A., Otlewski, J., and Krężel, A. (2010) The high Zn(II) affinity of the tetracysteine tag affects its fluorescent labeling with biarsenicals. *ChemBioChem* **11**, 1214–1218
25. Hoffmann, C., Gaietta, G., Zürn, A., Adams, S. R., Terrillon, S., Ellisman, M. H., Tsien, R. Y., and Lohse, M. J. (2010) Fluorescent labeling of tetracysteine-tagged proteins in intact cells. *Nat. Protoc.* **5**, 1666–1677
26. Schindelin, J., Arganda-Carreras, I., Frise, E., Kaynig, V., Longair, M., Pietzsch, T., Preibisch, S., Rueden, C., Saalfeld, S., Schmid, B., Tinevez, J. Y., White, D. J., Hartenstein, V., Eliceiri, K., Tomancak, P., and Cardona, A. (2012) Fiji: an open-source platform for biological-image analysis. *Nat. Methods* **9**, 676–682
27. Unzueta, U., Vázquez, F., Accardi, G., Mendoza, R., Toledo-Rubio, V., Giuliani, M., Sannino, F., Parrilli, E., Abasolo, I., Schwartz, S., Jr., Tutino, M. L., Villaverde, A., Corchero, J. L., and Ferrer-Miralles, N. (2015) Strategies for the production of difficult-to-express full-length eukaryotic proteins using microbial cell factories: production of human alpha-galactosidase A. *Appl. Microbiol. Biotechnol.* **99**, 5863–5874
28. Madani, F., Lind, J., Damberg, P., Adams, S. R., Tsien, R. Y., and Gräslund, A. O. (2009) Hairpin structure of a biarsenical-tetracysteine motif determined by NMR spectroscopy. *J. Am. Chem. Soc.* **131**, 4613–4615
29. Gaietta, G. M., Giepmans, B. N., Deerinck, T. J., Smith, W. B., Ngan, L., Llopis, J., Adams, S. R., Tsien, R. Y., and Ellisman, M. H. (2006) Golgi twins in late mitosis revealed by genetically encoded tags for live cell imaging and correlated electron microscopy. *Proc. Natl. Acad. Sci. USA* **103**, 17777–17782
30. Moriarty-Craige, S. E., and Jones, D. P. (2004) Extracellular thiols and thiol/disulfide redox in metabolism. *Annu. Rev. Nutr.* **24**, 481–509
31. Fessenden, J. D., and Mahalingam, M. (2013) Site-specific labeling of the type 1 ryanodine receptor using biarsenical fluorophores targeted to engineered tetracysteine motifs. *PLoS One* **8**, e64686
32. Higuchi, K., Yoshimitsu, M., Fan, X., Guo, X., Rasaiah, V. I., Yen, J., Tei, C., Takenaka, T., and Medin, J. A. (2010) Alpha-galactosidase A-Tat fusion enhances storage reduction in hearts and kidneys of Fabry mice. *Mol. Med.* **16**, 216–221
33. Adams, S. R., Campbell, R. E., Gross, L. A., Martin, B. R., Walkup, G. K., Yao, Y., Llopis, J., and Tsien, R. Y. (2002) New biarsenical ligands and tetracysteine motifs for protein labeling in vitro and in vivo: synthesis and biological applications. *J. Am. Chem. Soc.* **124**, 6063–6076
34. Matsuura, F., Ohta, M., Ioannou, Y. A., and Desnick, R. J. (1998) Human α-galactosidase A: characterization of the N-linked oligosaccharides on the intracellular and secreted glycoforms overexpressed by Chinese hamster ovary cells. *Glycobiology* **8**, 329–339
35. Yam, G. H., Bosshard, N., Zuber, C., Steinmann, B., and Roth, J. (2006) Pharmacological chaperone corrects lysosomal storage in Fabry disease caused by trafficking-incompetent variants. *Am. J. Physiol. Cell Physiol.* **290**, C1076–C1082
36. Garman, S. C. (2007) Structure-function relationships in α-galactosidase A. *Acta Paediatr.* **96**, 6–16
37. Alexander, S. C., and Schepartz, A. (2014) Interactions of AsCy3 with cysteine-rich peptides. *Org. Lett.* **16**, 3824–3827

Received for publication January 23, 2017.
Accepted for publication July 31, 2017.